Asymptotic and leading correction-to-scaling specific-heat critical exponents and amplitudes for quench-disordered ferromagnets from resistivity measurements

S. N. Kaul* and M. Sambasiva Rao
School of Physics, University of Hyderabad, Central University Post Office, Hyderabad—500134, Andhra Pradesh, India
(Received 30 October 1990)

We report an experimental determination of the asymptotic and leading correction-to-scaling specific-heat critical exponents and amplitudes for quench-disordered ferromagnets. The renormalization-group estimates, available for some of the amplitude ratios only, are in agreement with the presently determined values. The scaling relation $\alpha^+=\alpha^-$ is obeyed and the asymptotic amplitude ratio A^+/A^- possesses a value *characteristic* of a three-dimensional isotropic nearest-neighbor Heisenberg ferromagnet with *isotropic long-range dipolar* interactions.

I. INTRODUCTION

Early electrical resistivity[1] (ρ), bulk magnetization[2–6] (BM), and ac susceptibility[7] (χ_{ac}) measurements performed on amorphous (a-) $Fe_xNi_{80-x}B_{19}Si_1$ alloys revealed that the critical exponents α, β, and γ, characterizing the behavior of the specific heat, C_p, spontaneous magnetization, and initial susceptibility near the ferromagnetic (FM)–paramagnetic (PM) phase transition, possess values ($\alpha\simeq-0.2$, $\beta\simeq0.4$, $\gamma\simeq1.31$, and $\delta\simeq4.4$) that are close to, but systematically shifted[4,5] away from, those ($\alpha\simeq-0.11$, $\beta\simeq0.365$, $\gamma\simeq1.386$, and $\delta\simeq4.8$) theoretically predicted for a three-dimensional (3D) isotropic nearest-neighbor (NN) Heisenberg ferromagnet. Such deviations from the predictions of 3D NN Heisenberg model have been tentatively attributed[5] to long-range isotropic dipolar or Ruderman-Kittel-Kasuya-Yosida (RKKY) interactions and/or isotropic Heisenberg interactions extending beyond the NN distance.[8,9] Subsequently, an elaborate analysis of highly accurate zero-field susceptibility (χ_{ac}) data[10] on the same alloy compositions yielded a true asymptotic value of the exponent γ that exactly matches[10] that predicted by renormalization-group (RG) theory[11] for pure (ordered) spin systems with space as well as spin dimensionality of 3 ($d=3$, $n=3$) and specific-heat critical exponent, $\alpha_p<0$. It was also demonstrated that systematic deviations in the case of the exponent γ observed previously are the artifacts of an analysis that completely neglects the correction-to-scaling (CTS) terms, and that some of the above-mentioned interactions, if present, play the role of an *irrelevant scaling field* in the RG sense (i.e., they give rise to corrections to the dominant singular behavior, leaving the leading singularity in the asymptotic behavior of the pure system unaltered). The ac susceptibility results, however, remain inconclusive as far as the effect of the *isotropic dipolar* long-range (IDL) interactions on the asymptotic critical behavior is concerned, because isotropic dipolar perturbation acts as a *relevant scaling field*[12] and shifts the asymptotic critical exponents away from their isotropic Heisenberg short-range (ISR) values by an amount that is so small (especially for β and γ) as to fall well within the error limits of the experimentally determined exponent values. Considering the theoretical prediction[12] that the IDL values of the exponents α and γ deviate from their ISR counterparts by as much as 8% and 0.5%, respectively, it should, in principle, be possible to determine experimentally the change in the leading singularity caused by IDL interactions with greater ease from the C_p (more so from[5] ρ) measurements than from χ_{ac} measurements. The origin of systematic deviations in the case of the exponent γ suggests that the previously determined values of the exponent α are not the true asymptotic values, and that a reanalysis, which takes into account the confluent singularity terms, of the earlier resistivity data[1] is called for. The futility of such an exercise is, however, apparent in view of the poor resolution (10 ppm) achieved previously[1] and the absence of a sharp anomaly[1] in $d\rho/dT$ at the Curie point, T_c. In retrospect, the most likely causes for a smeared transition[1] at T_c seem to be (i) that the three-point differentiation method used to determine $d\rho/dT$ from the $\rho(T)$ data taken at 1 K intervals leads to some sort of averaging over a temperature region as wide as 2 K, (ii) that the temperature drift rate of 0.6 K/min used to measure $\rho(T)$ is not slow enough to ensure that the measured resistivity values are characteristic of spin system in thermal equilibrium, especially for temperatures in the immediate vicinity of T_c, and (iii) the sizable magnitude of the temperature gradient along the length of the sample and the stresses introduced during thermal cycling. Furthermore, earlier $d\rho/dT$ data[1] could be fitted to a 3D Heisenberg-like value of α up to $\epsilon=(T-T_c)/T_c\simeq0.3$, as contrasted to the BM and χ_{ac} data, which reveal that the exponent γ assumes a 3D Heisenberg-like value only for $\epsilon\lesssim0.05$. Foregoing remarks prompted us to undertake detailed resistivity measurements on amorphous $Fe_xNi_{80-x}B_{19}Si$ alloys with $x=10$, 13, and 16.

II. EXPERIMENTAL DETAILS

In order to facilitate an accurate determination of the asymptotic and leading correction-to-scaling specific-heat critical exponents and amplitudes for these alloys, highly accurate (the relative accuracy better than 1 ppm) resistivity data, using the four-probe dc method, have been taken on amorphous $Fe_xNi_{80-x}B_{19}Si$ ($x=10$, 13, and 16) alloy ribbons of dimensions $0.04\times2\times60$ mm^3, prepared by the single-roller melt-quenching technique, at temperatures $\simeq30$ mK apart in the range $-0.1\leq\epsilon\leq0.1$ and at temperature intervals varying from 100 mK to 1 K outside this temperature range, keeping the sample temperature constant to within ±10 mK by means of a proportional integral and derivative (PID) temperature controller. Such a high accuracy in the resistivity measurements was achieved by a design of the sample holder, heater, and cryostat (details to be published elsewhere), which eliminates the stress-induced specious effects by allowing the alloy ribbons to expand and contract freely during thermal cycling and ensures that the temperature difference between the ends of the sample does not exceed 20 mK in any case. The sample temperature was monitored by a precalibrated Pt resistance sensor, while the temperature gradient across the length of the sample was measured by precalibrated copper-constantan thermocouples connected in the differential mode. Note that the earlier[10] $\chi_{ac}(T)$ and the present $\rho(T)$ measurements have been performed on the adjacent pieces of the same alloy ribbons. A detailed compositional analysis[10] of a number of alloy strips coming from the same batch revealed that the change in Fe concentration, x, per unit length, $dx/dl\leq0.003$ at. % cm^{-1}. In view of our earlier finding that, within the composition range of present interest, T_c varies with x as[1-3,13] $dT_c/dx\simeq26$ K/at. % and the fact that the distance between the voltage probes is $\simeq1$ cm, the concentration fluctuations in the sample would give rise to a fluctuation in T_c of the order of $\delta T_c\simeq0.08$ K. Therefore, the data taken in the reduced temperature range $\epsilon\leq\delta T_c/T_c$ have been left out of the data analysis. Resistivity data collected during different experimental runs on the same samples or on different samples taken from the same alloy batch reveal that the absolute values of the normalized resistivity, $\rho(T)/\rho(T_c)$, could be reproduced to within 1%; the T_c values used were those determined from the previous[10] χ_{ac} measurements.

III. RESULTS AND DATA ANALYSIS

The temperature derivative of resistivity (evaluated by the three-point differentiation method) normalized to the value of resistivity at T_c, $(d\rho/dT)/\rho(T_c)\equiv\alpha_r$, as a function of temperature in the reduced temperature range $-0.4\leq\epsilon\leq0.6$ for a-$Fe_xNi_{80-x}B_{19}Si$ alloys is shown in the inset of Fig. 1. It is noticed from the inset that

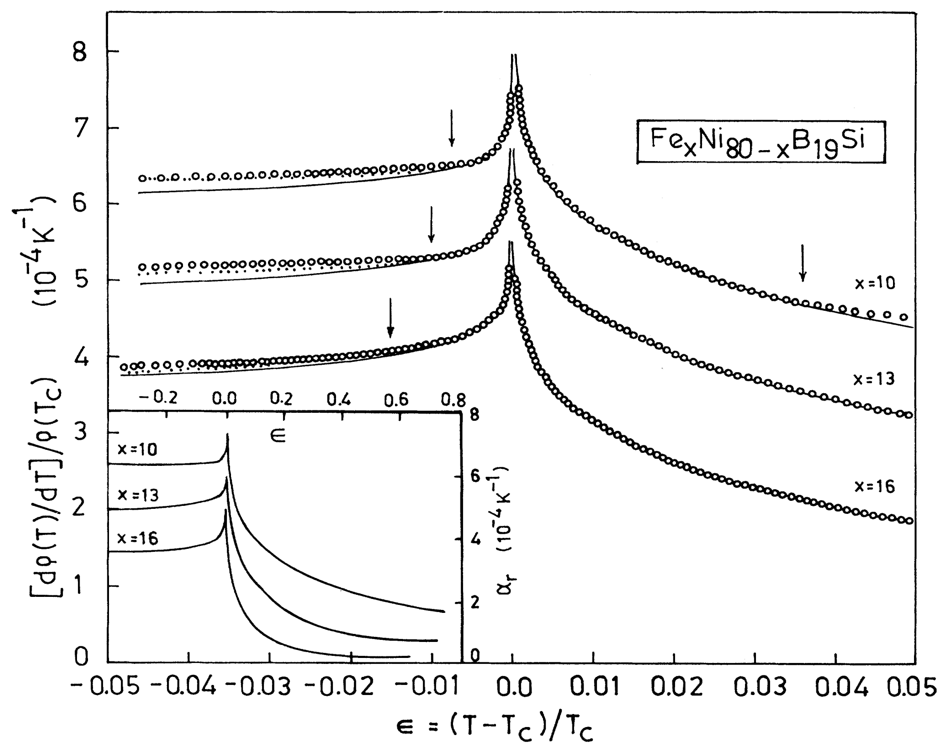

FIG. 1. $[1/\rho(T_c)](d\rho/dT)$ vs ϵ in the range $-0.05\leq\epsilon=(T-T_c)/T_c\leq0.05$. The solid and dotted curves through the data points are theoretical fits based on Eq. (1), see text. The downward arrows indicate the temperature beyond which the continuous curves deviate from the data. For the sake of clarity, only one-eighth of the total number of data points are shown in this figure, and the data points for the temperatures in close proximity to T_c are deleted. Inset shows $\alpha_r\equiv[d\rho/dT]/\rho(T_c)$ plotted against ϵ over a much wider temperature range. Note that in both the main figure and inset, the zero on the ordiante scale should read as 1 and 2, respectively, for the alloys with $x=13$ and 16.

scatter in the earlier[1] data is practically absent in the new set of data, and that $\alpha_r(T)$ now exhibits a sharp singularity at T_c; otherwise, the present results preserve all the essential features of the previously published[1] data. The T_c values used in constructing the plots shown in Fig. 1 have been determined by the analysis that includes the CTS confluent singularity terms and whose details are given in Sec. III B.

Renormalization-group theories[14-17] dealing with quench-disordered spin systems reveal that the quenched disorder in $d=n=3$ ISR spin system acts as an *irrelevant scaling* field, in that an additional leading confluent correction term, characterized by the exponent[10,12,16,17] $\Delta_1=|\alpha_p|$, appears in the expression for C_p or $d\rho/dT$, besides the one present in pure systems and involving the exponent Δ_2. The so-called "conventional" RG theories[14-17] thus predict a temperature dependence for α_r for temperatures not too close to T_c as

$$\frac{1}{\rho(T_c)}\frac{d\rho(T)}{dT}=\frac{A^{\pm}}{\alpha^{\pm}}(\pm\epsilon)^{-\alpha^{\pm}}[1+a_{c_1}^{\pm}\alpha^{\pm}(\pm\epsilon)^{\Delta_1}+a_{c_2}^{\pm}\alpha^{\pm}(\pm\epsilon)^{\Delta_2}]-\frac{A^{\pm}}{\alpha^{\pm}}+B^{\pm}\ , \qquad (1)$$

where the plus and minus signs denote temperatures above and below T_c, and $A^{\pm}$ $(a_{c_1}^{\pm},a_{c_2}^{\pm})$ and $\alpha^{\pm}(\Delta_1,\Delta_2)$ are the asymptotic (leading correction-to-scaling) critical amplitudes and critical exponents, respectively. By contrast, the so-called "unconventional" RG theory[18] claims that in the presence of quenched disorder the pure fixed point is not stable even for systems with $\alpha_p<0$, that the critical exponents depend on composition x, and as $x\rightarrow x_c$ (percolation threshold), they approach the Fisher-renormalized values.

A. Pure power-law analysis

Despite the fact that the single-power-law analysis[1-7] of our earlier ρ, BM, and χ_{ac} data taken in the critical region clearly demonstrates that, contrary to the predictions of the so-called "unconventional" RG theory, the 3D pure Heisenberg fixed point is stable even when short-ranged quenched disorder is present, we repeat this analysis for the present data because of the serious problems that our earlier resistivity data suffer from. Thus, to begin with, we fit the resistivity data for $T<T_c$ and $T>T_c$ separately to a pure power law by setting $a_{c_1}^{\pm}=a_{c_2}^{\pm}=0$ in Eq. (1) and using a range-of-fit analysis wherein change, if any, in the values of the fitting parameters $A^{\pm}$, $B^{\pm}$, $\alpha^{\pm}$, and $T_c^{\pm}$ is monitored as the temperature range[19] ($\epsilon_{min}\le\epsilon\le\epsilon_{max}$) of the fit is narrowed down by raising (lowering) ϵ_{min} (ϵ_{max}) toward ϵ_{max} (ϵ_{min}) while keeping ϵ_{max} (ϵ_{min}) fixed at a given value. The variation of various parameters with ϵ_{min} and ϵ_{max} is depicted in Figs. 2 and 3. The main results of this analysis are (a) $T_c^-\simeq T_c^+$ and $\alpha^-\simeq\alpha^+$ within the error limits; (b) the exponent α assumes a constant value in a narrow temperature interval $|\epsilon_{min}^{\pm}|\le\epsilon\le|\epsilon_{max}^{\pm}|$ only and increases with the Fe content from $\alpha=-0.15\pm0.015$ for $x=10$ to $\alpha=-0.11\pm0.015$ for $x=16$ (this result is at variance with our earlier finding[1] that the $d\rho/dT$ data fit to a 3D Heisenberg-like value of α for $\epsilon^+\lesssim0.3$); and (c) $A^+/A^-\simeq1.55$ and

$$[B^+-(A^+/\alpha^+)]/[B^--(A^-/\alpha^-)]\simeq1.6\ .$$

Failure of the data to permit equality between $B^--(A^-/\alpha^-)$ and $B^+-(A^+/\alpha^+)$, which is dictated by the requirement that for $\alpha<0$, $d\rho^-/dT=d\rho^+/dT$ at $T=T_c$, emphasizes the necessity of including the confluent singularity terms in the analysis.

B. Analysis with confluent singularity terms

The parameters $a_{c_1}^{\pm}$, $a_{c_2}^{\pm}$, $\Delta_1^{\pm}$, and $\Delta_2^{\pm}$ in Eq. (1) are now permitted to be finite and possess different values for $T<T_c$ and $T>T_c$, and an effort is made to extract the values of $A^{\pm}$, $B^{\pm}$, $\alpha^{\pm}$, $a_{c_1}^{\pm}$, $a_{c_2}^{\pm}$, $\Delta_1^{\pm}$, $\Delta_2^{\pm}$, and $T_c^{\pm}$ by

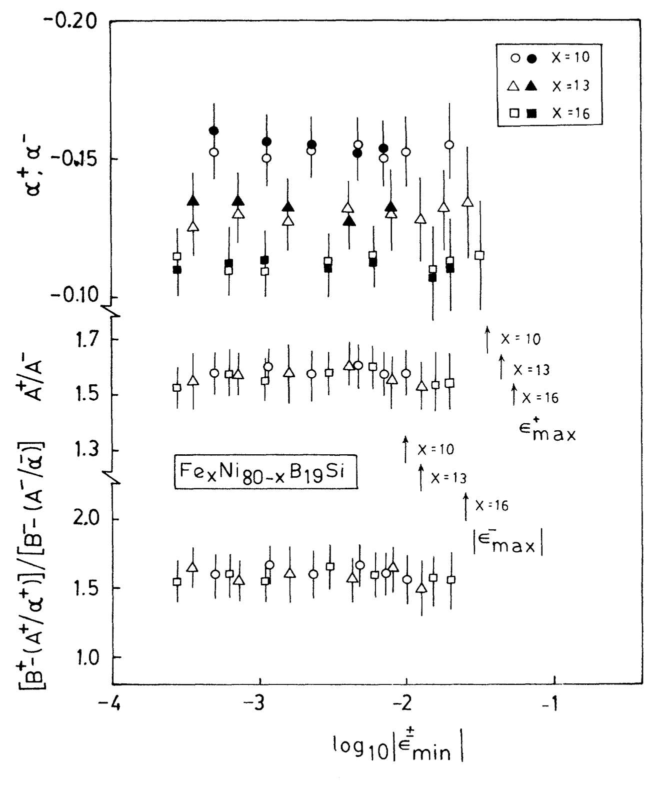

FIG. 2. Values for α^+, α^-, A^+/A^-, and $[B^+-(A^+/\alpha^+)]/[B^--(A^-/\alpha^-)]$ obtained from a fit of the data to Eq. (1) for various $|\epsilon_{min}^{\pm}|$ with the constraint $a_{c_1}^{\pm}=a_{c_2}^{\pm}=0$. Solid and open symbols refer to the parameter values obtained for temperatures below and above T_c, respectively.

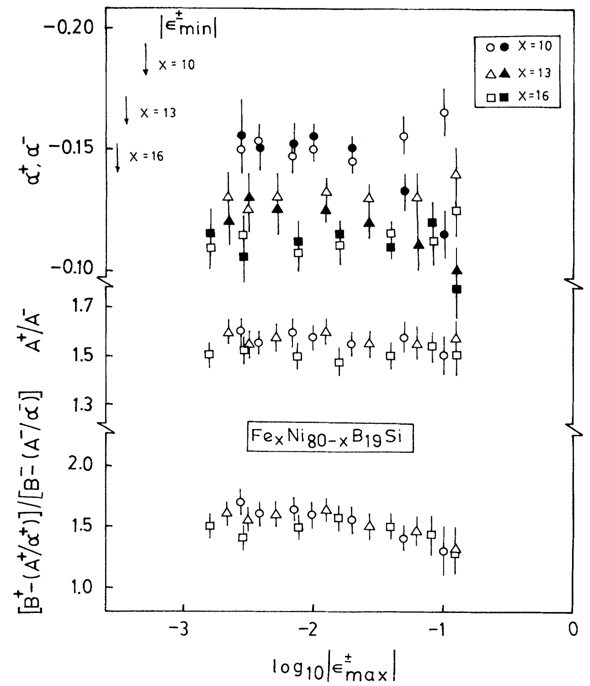

FIG. 3. Values for α^+, α^-, A^+/A^-, and $[B^+-(A^+/\alpha^+)]/[B^- -(A^-/\alpha^-)]$ obtained from least-squares fits to the data based on Eq. (1) for various $|\epsilon^{\pm}_{max}|$ with the constraint $a^{\pm}_{c_1}=a^{\pm}_{c_2}=0$. Symbols have the same meaning as in Fig. 2.

fitting α_r data to Eq. (1) for $T<T_c$ and $T>T_c$ separately, using the range-of-fit analysis and a nonlinear least-squares-fit computer program that treats $A^{\pm}$, $B^{\pm}$, $\alpha^{\pm}$, $a^{\pm}_{c_1}$, $a^{\pm}_{c_2}$, and $T^{\pm}_c$ as free-fitting parameters, but keeps (Δ^+_1,Δ^+_2) and (Δ^-_1,Δ^-_2) pairs fixed at a given value in the ranges $0.01 \le \Delta^{\pm}_1 \le 0.20$ and $0.35 \le \Delta^{\pm}_2 \le 0.75$, respectively. The same procedure is repeated for another fixed value of the pair, which differs from the previous one by $(\pm 0.01, \pm 0.01)$. Best fits, as inferred from the smallest value of the sum of the deviation squares, χ^2, are obtained for $\Delta^+_1=\Delta^-_1=0.11\pm0.06$, and $\Delta^+_2=\Delta^-_2=0.54 \pm 0.10$, with the parameter values that have an undesirably large uncertainty but are otherwise close to those determined by the following procedure and listed in Table I. The values of $\Delta^{\pm}_1$ and $\Delta^{\pm}_2$ so obtained conform very well with those ($\Delta_1=0.115\pm0.009$ and $\Delta_2=0.550\pm0.016$) predicted by RG theories,[11,12] as well as with the best theoretical estimates of exponents Δ_1 and Δ_2 presently available,[17] i.e., $\Delta_1=0.09$, and $\Delta_2=0.048$. Realizing that the large uncertainty mainly results from the correlation between different parameters in a multiparameter fit, and that the above values of Δ_1 and Δ_2 embrace more accurate values of $\Delta_1=0.11\pm0.05$, and $\Delta_2=0.55\pm0.05$, determined[10] from previous χ_{ac} measurements, a substantial reduction in the uncertainty is achieved by imposing the conditions $\Delta^+_1=\Delta^-_1, \Delta^+_2=\Delta^-_2$, and $T^+_c=T^-_c$, and by holding the values of $\Delta^{\pm}_1$ and $\Delta^{\pm}_2$, and T^-_c constant at $\Delta^{\pm}_1=0.11$, $\Delta^{\pm}_2=0.55$, and T^+_c [the value of T^+_c is more reliable since, Eq. (1) provides an ex-

TABLE I. Values of the specific-heat asymptotic critical exponents, asymptotic critical amplitudes, and correction-to-scaling amplitudes for amorphous $Fe_xNi_{80-x}B_{19}Si$ alloys deduced by least-squares fitting the experimental data in the specified temperature ranges (continuous curves in Fig. 1) to Eq. (1) of the text. Relevant parameter values determined previously from the ac susceptibility data are also included for the sake of completeness. Numbers in parentheses denote uncertainty in the least significant figure. ACS denotes ac susceptibility and PW, present work.

X (at. %)	Reference	Method	$T^-_c=T^+_c$	Range for fit: ϵ^-_{min} $[\epsilon^+_{min}]$ (10^{-3})	ϵ^-_{max} $[\epsilon^+_{max}]$ (10^{-3})	A^- $[A^+]$ $(10^{-3}\ K^{-1})$	B^- $[B^+]$ $(10^{-3}\ K^{-1})$	α^- $[\alpha^+]$	$a^-_{c_1}$ $[a^+_{c_1}]$	$a^-_{c_2}$ $[a^+_{c_2}]$	$[a^+_{\chi_1}]$	$[a^+_{\chi_2}]$	χ^2 (10^{-10})
10	PW	$d\rho/dT$	187.03(5)	−7.50	−0.50	0.075(1)	0.330(5)	−0.114(5)	2.80(60)	−1.40(65)			0.76
				[0.50]	[36.00]	[0.116(1)]	[0.161(2)]	[−0.114(5)]	[0.23(5)]	[−1.45(25)]			1.48
	10	ACS	187.06(7)	[0.82]	[34.00]						[0.030(10)]	[0.32(4)]	
13	PW	$d\rho/dT$	268.64(6)	−10.00	−0.37	0.073(1)	0.335(5)	−0.115(5)	2.45(65)	−2.45(65)			0.95
				[0.35]	[45.00]	[0.110(1)]	[0.155(2)]	[−0.113(5)]	[0.25(5)]	[−2.45(25)]			0.99
	10	ACS	268.62(8)	[0.67]	[41.00]						[0.030(10)]	[0.48(4)]	
16	PW	$d\rho/dT$	341.45(5)	−20.00	−0.29	0.071(1)	0.305(5)	−0.111(5)	3.50(50)	−2.75(75)			1.11
				[0.28]	[55.00]	[0.105(1)]	[0.130(2)]	[−0.110(5)]	[0.38(7)]	[−2.85(25)]			1.13
	10	ACS	341.41(6)	[0.53]	[55.00]						[0.068(12)]	[0.63(7)]	

cellent fit to the data over a much wider temperature range for $T > T_c$ than for $T < T_c$; see Fig. 1], respectively. With these constraints, a range-of-fit analysis of the data has been carried out separately for temperatures below and above T_c, and the results of this analysis are shown in Figs. 4–7. Consistent with the outcome of the pure-power-law analysis, the best least-squares (LS) fits to the data based on Eq. (1) can be obtained only in a narrow temperature range around T_c (Table I); but now χ^2 is reduced by two orders of magnitude. A visual demonstration of the quality of such fits is provided by Fig. 1, in which the α_r data (open circles) are plotted against ϵ in a restricted temperature range of $-0.05 \le \epsilon \le 0.05$, and the theoretical fits in the specified temperature ranges (Table I), based on Eq. (1) with parameter values given in Table I, are denoted by the solid curves. The main points that emerge from the range-of-fit analysis (Figs. 4–7) are as follows. (i) The parameter values widely differ from those listed in Table I if the data outside the temperature range $|\epsilon_{\text{min}}^{\pm}| \le \epsilon \le |\epsilon_{\text{max}}^{\pm}|$ are also included in the analysis and the quality of such fits deteriorates rapidly, as inferred from the increased value of χ^2. To elucidate this point further, if the above type of fits are attempted over a temperature range $-0.05 \le \epsilon \le 0$ (shown in Fig. 1 by dotted curves), A^- remains practically unaltered, α^- ($\simeq -0.07$) and $a_{c_1}^-$ increase by a factor ~ 2, $a_{c_2}^- \approx 0$, and B^- reduces by a factor ~ 3. Such a drastic change in the parameter values, especially for the $T < T_c$ fits, is related to the fact that α_r exhibits a plateau (roughly) for $T < T_c$ and is a

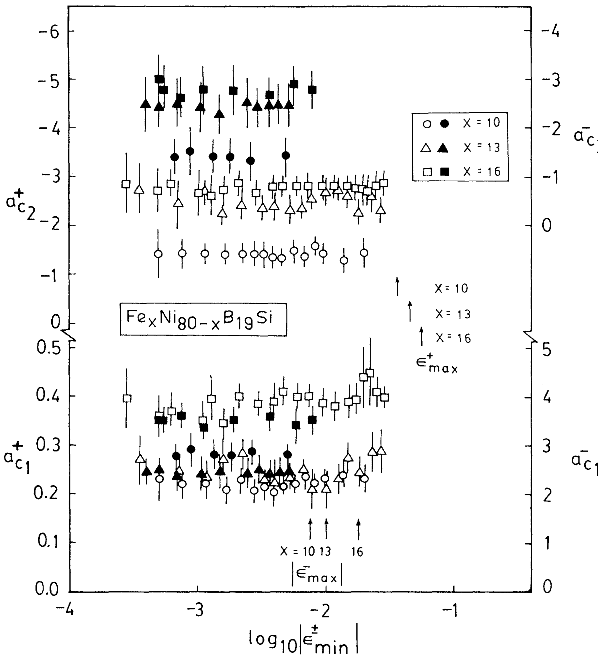

FIG. 5. Values for $a_{c_1}^+$, $a_{c_1}^-$, $a_{c_2}^+$, and $a_{c_2}^-$ deduced from fits to the data based on Eq. (1) for various $|\epsilon_{\text{min}}^{\pm}|$ with the constraints $T_c^+ = T_c^-$, $\Delta_1^+ = \Delta_1^- = 0.11$, and $\Delta_2^+ = \Delta_2^- = 0.55$. Errors bars, when omitted, are comparable to or smaller than the size of the data symbol. Symbols have the same meaning as in Fig. 4.

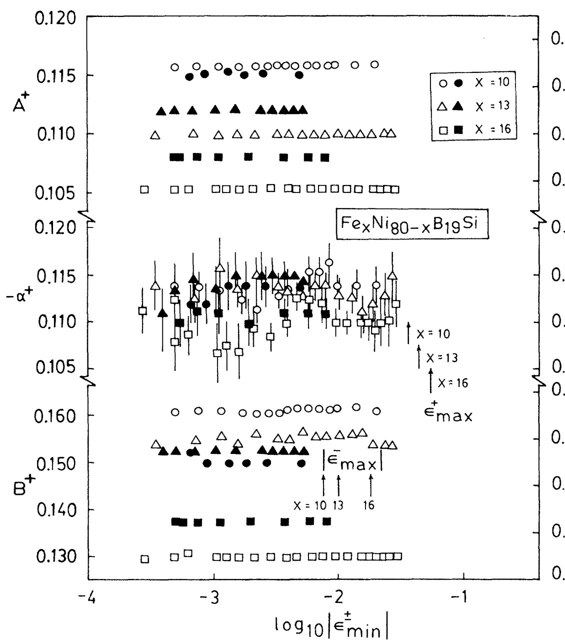

FIG. 4. Values for α^+, α^-, A^+, A^-, B^+ and B^- obtained by fitting the data to Eq. (1) for various $|\epsilon_{\text{min}}^{\pm}|$ with the constraints $T_c^+ = T_c^-$, $\Delta_1^+ = \Delta_1^- = 0.11$, and $\Delta_2^+ = \Delta_2^- = 0.55$. Error bars, when omitted, are comparable to or smaller than the size of the data symbol. Solid and open symbols refer to the parameter values obtained for temperatures below and above T_c, respectively.

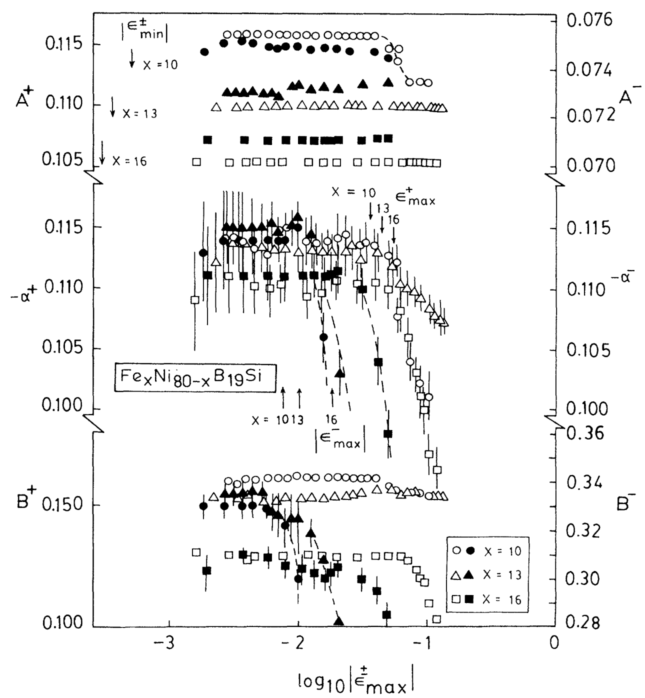

FIG. 6. Values for α^+, α^-, A^+, A^-, B^+, and B^- obtained by fitting the data to Eq. (1) for various $|\epsilon_{\text{max}}^{\pm}|$ with the constraints $T_c^+ = T_c^-$, $\Delta_1^+ = \Delta_1^- = 0.11$, and $\Delta_2^+ = \Delta_2^- = 0.55$. Error bars, when omitted, are comparable to or smaller than the size of the data symbol. Solid and open symbols refer to the parameter values obtained for temperatures below and above T_c, respectively.

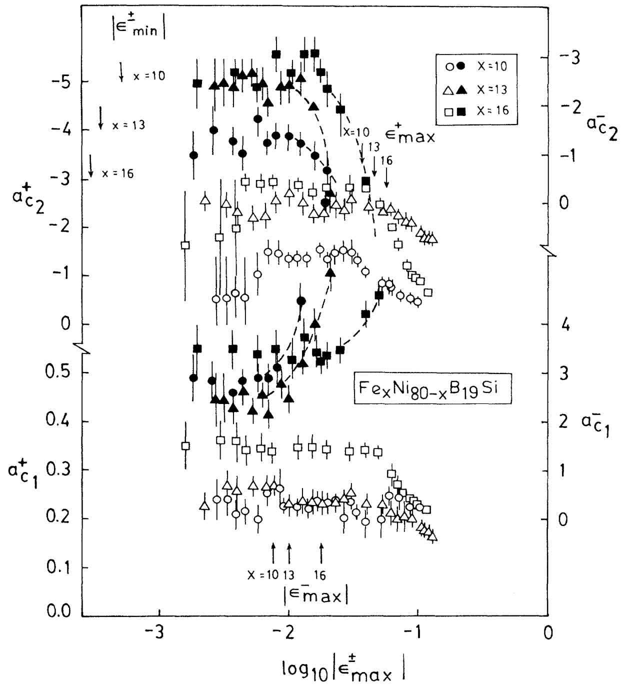

FIG. 7. Values for $a^{+}_{c_1}$, $a^{-}_{c_1}$, $a^{+}_{c_2}$, and $a^{-}_{c_2}$ deduced from fits to the data based on Eq. (1) for various $|\epsilon^{\pm}_{max}|$ with the constraints $T_c^{+}=T_c^{-}$, $\Delta_1^{+}=\Delta_1^{-}=0.11$, and $\Delta_2^{+}=\Delta_2^{-}=0.55$. Error bars, when omitted, are comparable to or smaller than the size of the data symbol. Symbols have the same meaning as in Fig. 4.

consequence of a strong interplay[1,9] between the electron-magnon scattering and the scattering of conduction electrons from the critical fluctuations of magnetization. (ii) The exponents $\alpha^{\pm}$ increase toward the mean field value ($\alpha^{\pm}=0$) for $\epsilon > |\epsilon^{\pm}_{max}|$. (iii) The correction-to-scaling term involving the exponent Δ_1 (Δ_2) becomes important only for temperatures in the immediate vicinity of T_c (not too close to T_c), as is evident from the finding that χ^2 remains practically unaltered despite large variation in the value of the CTS amplitude $a^{\pm}_{c_2}$ ($a^{\pm}_{c_1}$) for temperatures $\epsilon \simeq 0$ ($|\epsilon| > 0$). The percentage deviation of the data from the best fit is plotted as a function of reduced temperature ϵ in Fig. 8. The data exhibit considerable departure from the best fits for temperatures $|\epsilon| < |\epsilon^{\pm}_{min}|$ and $|\epsilon| > |\epsilon^{\pm}_{max}|$. While the deviations for temperatures $|\epsilon| < |\epsilon^{\pm}_{min}|$ are a manifestation of the "rounding" caused primarily by sample inhomogeneities (composition fluctuations and/or gradients, cf. Sec. II) and to a lesser extent by the averaging introduced by the three-point differentiation method, temperature gradients across the sample length, and the Earth's magnetic field, the deviations for $\epsilon > \epsilon^{+}_{max}$ signal a crossover[5] from the pure to random behavior.

IV. COMPARISON WITH THEORY AND OTHER EXPERIMENTS

Table II compares the presently determined values of the ratios involving asymptotic and CTS critical ex-

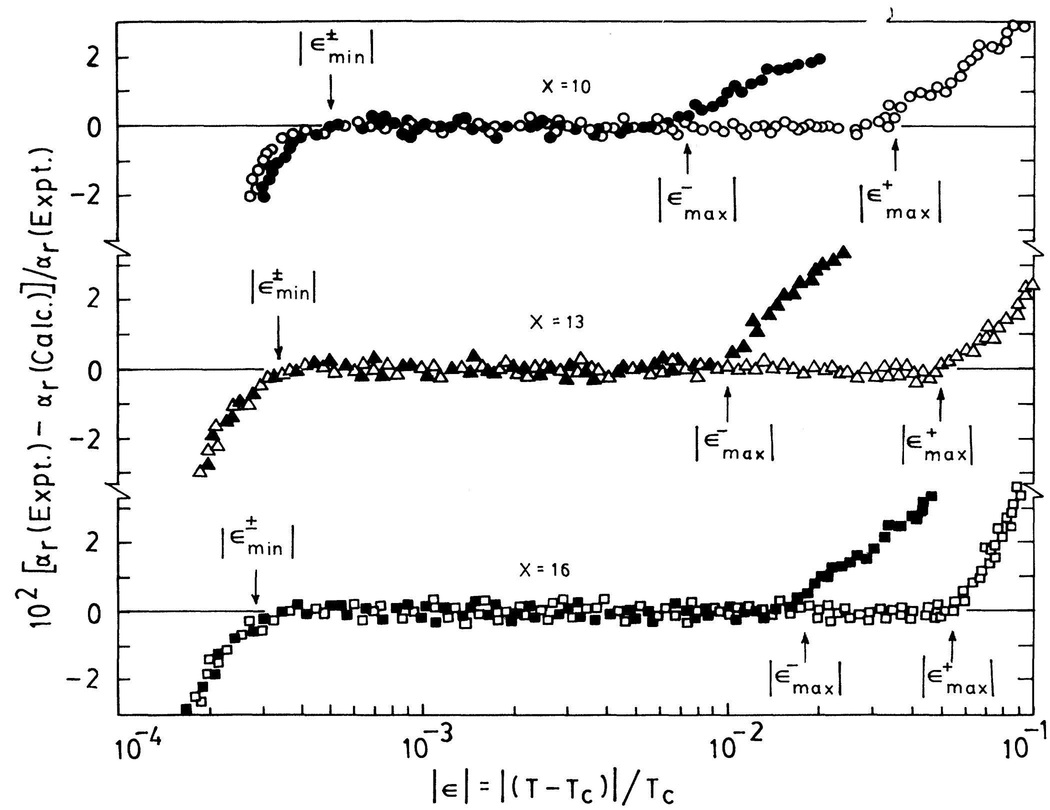

FIG. 8. Percentage deviation of the data from the best least-squares fits. Solid symbols, $\epsilon < 0$; open symbols, $\epsilon > 0$. The arrows indicate $|\epsilon^{\pm}_{min}|$ and $|\epsilon^{\pm}_{max}|$.

TABLE II. Comparison between the experimentally determined and theoretically estimated values for the ratios involving asymptotic critical exponents, critical amplitudes, and correction-to-scaling amplitudes. Numbers in parentheses denote uncertainty in the least significant figure arising from standard errors. ACS denotes ac susceptibility; PW, present work; and RG, renormalization group.

Material	Reference	Method	α^+	α^+/α^-	A^+/A^-	$(B^+ - A^+/\alpha^+)/(B^- - A^-/\alpha^-)$	$a_{c_1}^+/a_{c_1}^-$	$a_{c_2}^+/a_{c_2}^-$	$a_{c_1}^+/a_{\chi_1}^+$	$a_{c_2}^+/a_{\chi_2}^+$
$X=10$	PW	$d\rho/dT$	−0.114(5)	1.00(9)	1.54(3)	1.17(15)	0.08(4)	1.04(50)	7.7(50)	4.5(10)
	10	ACS								
$X=13$	PW	$d\rho/dT$	−0.113(5)	0.98(9)	1.51(3)	1.16(15)	0.10(5)	1.00(50)	8.3(50)	5.1(10)
	10	ACS								
$X=16$	PW	$d\rho/dT$	−0.110(5)	0.99(9)	1.49(3)	1.15(15)	0.11(4)	1.03(40)	5.6(26)	4.5(10)
	10	ACS								
3D Heisenberg	20	RG, $\vartheta(\varepsilon)$ perturbative expansion		1.00	1.36	1.00				
	11, 21–23	RG, $\vartheta(\varepsilon^2)$ perturbative expansion	−0.115(9)	1.00(15)	1.24	1.00		1.75[a]		4.6(5)
	12, 23–25	RG, ε-recursion	−0.125	1.00	1.50[b]	1.00		1.00[c]		4.4
	12	RG, ε-expansion dipole perturbation	−0.135	1.00	1.54[b]	1.00		1.00[c]		

[a]Value obtained when only the terms up to first order in ε ($=4-d$) are retained (Ref. 22); when the terms second order in ε are also considered, the ratio assumes a very large *negative* (Ref. 22) value.

[b]Value computed from the relation (Ref. 24) $A^+/A^- \approx 1-4\alpha$ when the value of α given in the fourth column of this table is used.

[c]Value obtained to the leading order in ε from the relation (Ref. 25) $a_c^+/a_c^- = (\alpha^+/\alpha^-) = 1.00$.

ponents and amplitudes with those predicted by the RG theories[11,12,20–24] for pure $d=n=3$ spin systems with or without IDL interactions. The salient features of the data presented in Tables I and II are the following: (i) Values of the asymptotic and CTS critical exponents and amplitudes for both C_p and χ_{ac} have been extracted from the least-squares fits which employ roughly the same temperature range for a given sample; (ii) $(T_c)_\rho=(T_c)_{\chi_{ac}}$ for all the alloys in question; (iii) the scaling relation $\alpha^-=\alpha^+$ is obeyed to a high degree of accuracy; (iv) consistent with $\alpha<0$, the ratio $(B^+-A^+/\alpha^+)/(B^--A^-/\alpha^-)\approx 1$; (v) exponent α and the ratios involving asymptotic and CTS amplitudes for susceptibility and/or specific heat *do not* depend on composition; (vi) the amplitude ratios $a_{c_1}^+/a_{c_1}^-$ and $a_{c_1}^+/a_{\chi_1}^+$ seem to possess universal values, but more results are needed to establish this point; and (vii) the experimental values for α, A^+/A^-, $a_{c_2}^+/a_{c_2}^-$, and $a_{c_2}^+/a_{\chi_2}^+$ conform very well with the RG estimates for the pure $n=d=3$ spin system with ISR and/or IDL interactions, but this agreement should be regarded with caution in view of the fact that the reliability of the numbers obtained through an extrapolation of the RG ε-expansion results to $\varepsilon=4-d=1$ is often hard to assess. For instance, the difference between the values of leading ISR exchange and IDL specific-heat exponents[1] (i.e., $\alpha_{IDL}-\alpha_{ISR}=-0.135+0.125=-0.010$) is *as significant as* that between $\alpha_{ISR}=-0.125$, and the more accurate value given by the renormalized ϕ^4 field theory,[11] $\alpha_{ISR}=-0.115$. Similarly, the RG calculations, based on the ε-recursion method, available only to the zeroth order in $4-d$, yield[25] for $d=3$ the value $a_{c_2}^+/a_{c_2}^-=1$ for both ISR and IDL fixed points, whereas a perturbative expansion RG treatment[22] of the pure ISR system gives to the order ε, $a_{c_2}^+/a_{c_2}^-=1.75$. Thus the role of IDL interactions, if present, can be assessed better by comparing the values given in Table II with those reported for pure $n=d=3$ spin systems with or without IDL interactions rather than with the theoretical values whose reliability is in doubt. Unfortunately, accurate values have been experimentally determined only for the exponent α and the ratio A^+/A^-. An ideal example of a pure ISR exchange $n=d=3$ system is provided by the antiferromagnet $RbMnF_3$ because dipolar forces are absent[26] in antiferromagnets. Another ideal but extreme case in which dipolar forces are present in addition to the isotropic Heisenberg exchange is the ferromagnet EuS. A comparison of the values[27,28] $\alpha=-0.10$ and $A^+/A^-=1.28\pm0.02$ for $RbMnF_3$ (Ref. 27), and $\alpha=-0.124\pm0.016$ and $A^+/A^-=1.54\pm0.09$ for EuS (Ref. 28), with those listed in Table II demonstrates that our value of α is the same (within the error limits) as those reported[27,28] for $RbMnF_3$ and EuS, but the A^+/A^- ratio closely agrees only with the value given for EuS. In view of the observation[13] that the alloys with $x<x_c$ ($\simeq 3$) exhibit spin-glass behavior, long-range RKKY interactions are expected to be present in association with dominantly large direct nearest-neighbor Heisenberg exchange interactions in the glassy alloys under consideration for which $x>x_c$. The present results do not, however, permit us to draw a definite conclusion regarding the effect of RKKY interactions on the critical behavior, presumably because the isotropic short-range critical behavior is preserved[29] in the presence of RKKY interactions.

V. CONCLUSION

Consistent with the predictions of the RG theories,[11–26,20–25] our results allow us to conclude that IDL interactions *do affect* the asymptotic critical behavior in the glassy ferromagnets in question, and their presence is mainly felt through the enhanced value of the A^+/A^- ratio, i.e., $(A^+/A^-)_{IDL}>(A^+/A^-)_{ISR}$ (the IDL interactions leave other universal quantities practically unaltered from their values in the ISR case). Other important conclusions, based on the above observations (i)–(vii), are the following: (a) Quenched disorder does not affect the sharpness of the FM-PM phase transition and the critical behavior if $\alpha<0$ for the pure system in which ISR exchange occurs in associated with IDL interactions; (b) asymptotic and CTS critical exponents and the amplitude ratios remain unaltered as the tricritical point[10,13] ($x_c\simeq 3$) is approached along the FM-PM phase transition line of the magnetic phase diagram; and (c) since a *crossover* to a random fixed point, characterized by a set of *new* critical exponents whose values *substantially* differ from the 3D Heisenberg ones, has *not* been observed for temperatures as close to T_c as $\epsilon\simeq 10^{-4}$, *anisotropic dipolar* interactions and *isotropic long-range exchange* interactions of the form $-(J_\infty/r^{d+\sigma})\mathbf{S}_0\cdot\mathbf{S}_r$, where $0<\sigma<2$ and $\sigma<2-\eta$ (which render the ISR Heisenberg fixed-point unstable), both are *absent* in the glassy alloys under consideration.

ACKNOWLEDGMENTS

The financial assistance by the Department of Science and Technology, New Delhi, under the Project No. SP/S2/M21/86 to carry out this work is gratefully acknowledged. One of us (M.S.R.) is thankful to the Department of Atomic Energy, India, for financial assistance.

---

*To whom all the correspondence should be addressed.

[1] G. Böhnke, S. N. Kaul, W. Kettler, and M. Rosenberg, Solid State Commun. **48**, 743 (1983).
[2] S. N. Kaul and M. Rosenberg, Philos. Mag. B **44**, 357 (1981).
[3] S. N. Kaul and M. Rosenberg, Solid State Commun. **41**, 857 (1982).
[4] S. N. Kaul, IEEE Trans. Magn. **MAG-20**, 1290 (1984).
[5] S. N. Kaul, J. Magn. Magn. Mater. **53**, 5 (1985).
[6] W.-U. Kellner, M. Fähnle, H. Kronmüller, and S. N. Kaul, Phys. Status Solidi B **144**, 397 (1987).
[7] S. N. Kaul, A. Hofmann, and H. Kronmüller, J. Phys. F **16**, 365 (1986).
[8] S. N. Kaul, Phys. Rev. B **24**, 6550 (1981).
[9] S. N. Kaul, Phys. Rev. B **27**, 5761 (1983).

[10]S. N. Kaul, Phys. Rev. B **38**, 9178 (1988).
[11]J. C. LeGuillou and J. Zinn-Justin, Phys. Rev. B **21**, 3976 (1980).
[12]A. Aharony, in *Phase Transitions and Critical Phenomena,* edited by C. Domb and M. S. Green (Academic, New York, 1976), Vol. 6, p. 357.
[13]S. N. Kaul, IEEE Trans. Magn. **MAG-17**, 1208 (1981).
[14]D. E. Khmel'nitzki, Zh. Eksp. Teor. Fiz. **68**, 1960 (1975) [Sov. Phys.—JETP **41**, 981 (1976)]; T. C. Lubensky, Phys. Rev. B **11**, 3573 (1975).
[15]G. Grinstein and A. Luther, Phys. Rev. B **13**, 1329 (1976).
[16]A. Weinrib and B. I. Halperin, Phys. Rev. B **27**, 413 (1983).
[17]G. Jug, Phys. Rev. B **27**, 609 (1983).
[18]G. Sobotta and D. Wagner, J. Magn. Magn. Mater. **49**, 77 (1985), and references cited therein.
[19]To facilitate the range-of-fit analysis, a fixed reference temperature T_0, which is nearly equal to T_c, is used to define the parameters $\epsilon_{\min} \equiv (T' - T_0)/T_0$ and $\epsilon_{\max} \equiv (T'' - T_0)/T_0$.
[20]E. Brezin, J. C. LeGuillou, and J. Zinn-Justin, Phys. Lett. **47A**, 285 (1974).
[21]C. Bervillier, Phys. Rev. B **14**, 4964 (1976).
[22]Mau-Chung Chang and A. Houghton, Phys. Rev. B **21**, 1881 (1980); Phys. Rev. Lett. **44**, 785 (1980).
[23]C. Bagnuls and C. Bervillier, Phys. Rev. B **24**, 1226 (1981).
[24]A. Aharony and P. C. Hohenberg, Phys. Rev. B **13**, 3081 (1976).
[25]A. Aharony and G. Ahlers, Phys. Rev. Lett. **44**, 782 (1980).
[26]M. E. Fisher and A. Aharony, Phys. Rev. Lett. **30**, 559 (1973).
[27]G. Ahlers and A. Kornblit, Phys. Rev. B **12**, 1938 (1975).
[28]A. Kornblit, G. Ahlers, and E. Buehler, Phys. Rev. B **17**, 282 (1978).
[29]R. Beutler and M. Fähnle, Phys. Rev. B **40**, 11 417 (1989).